Journal of Applied Electrochemistry **34**: 283–290, 2004.

An evaluation of electrolytic repair of discontinuous PVD copper seed layers in damascene vias

J.H. SUKAMTO, E. WEBB*, T. ANDRYUSHCHENKO and J. REID
Novellus Systems, 11155 SW Leveton Drive, Tualatin OR, 97062, USA
*(*author for correspondence, e-mail: Eric.Webb@novellus.com)*

Received 14 May 2003; accepted in revised form 14 October 2003

Key words: chip, copper, electrolytic, integrated-circuit, pyrophosphate, seed-repair, EDTA

Abstract

This paper presents a study of electrolytic repair of PVD seed using alkaline baths. The test features used were 6:1 aspect ratio (AR) 0.18 μm vias seeded with 250–1500 Å PVD. A wide variety of electrolytic repair process chemistry compositions and plating parameters were studied. The results showed that electrolytic repair of PVD seeds as thin as 500 Å could largely eliminate the bottom voids which otherwise result during subsequent plating in acidic baths. However, repair bath compositions and conditions conducive to optimum fill improvement have also resulted in rough (possibly pitted) wafer surfaces. It is believed that the electrolytic repair requirement of a high cathodic overpotential is in conflict with conditions yielding a smooth and defect-free surface on the submicron scale. Hydrogen evolution, corrosion of seed by complexing agent, and variable behaviour of copper oxide in the complexed alkaline repair baths are believed to contribute to the correlation of increased pitting and repair capability improvement. Therefore, electrolytic seed repair process appears to be a difficult and unpromising process for practical implementation.

1. Introduction

Previous work has shown that electroplating bath chemistry and waveform [1–5], the quality of PVD copper coverage [6], and the feature etch profile influence the maximum feature aspect ratio that can be successfully filled. Under optimum conditions, the capability to fill 0.1 μm trenches of 10:1 AR and 0.13 μm 6:1 AR vias has been reported.

When seed, electroplate, or etch conditions deviate from their optima, significantly less fill capability has been reported [1–6]. A loss of fill capability is usually manifested as either a centre void or a bottom void as shown in Figure 1. Centre voids result when the finite growth rate of copper growth near the feature neck is sufficient to pinch closed the feature prior to the completion of accelerated growth from the feature base. This void type is influenced by the initial feature shape, the plating bath capability to accelerate bottom-up growth within features, and the impact of seed coverage on initial copper growth in the features.

Bottom voids result when copper growth during the initial stages of electrodeposition is relatively slow near the feature base relative to elsewhere in the feature. In an acidic bottom-up fill bath, slow initial deposition near the feature base leads to fill acceleration above the feature base rather at the feature base. The result of fill acceleration beginning above the feature base is typically a void in the feature below the depth at which initial fill acceleration took place. Excessive agglomeration or poor coverage of PVD Cu on surfaces near the via base correlate to the formation of bottom voids. Plating conditions also modulate their severity [2]. Bottom voids in vias may lead to formation of opens in integrated circuits as these voids can migrate during subsequent wafer processing to fully obstruct a device current pathway.

Depending on the etch profile, smaller features of future device generations will require somewhat thinner PVD seeds to avoid pinch-off prior to or during electroplating. Because thinner seeds typically decrease PVD coverage near the via base, and thus increase bottom void formation, it is clear that new options for fill of future generation damascene features should be explored.

Numerous options which will extend Damascene fill by electrodeposition have been described. These include direct plate on barrier, PVD/CVD Cu bilayers, all CVD seed, barrier optimization to improve PVD Cu smoothness at low thickness, atomic layer deposition, wet process seed deposition [7], and augmentation of PVD seed using wet processes [6].

Electroless copper processes have been widely used in the electronics industry for decades, and their potential utility as a filling process for integrated circuits has been discussed [8]. Characteristics of electroless copper which

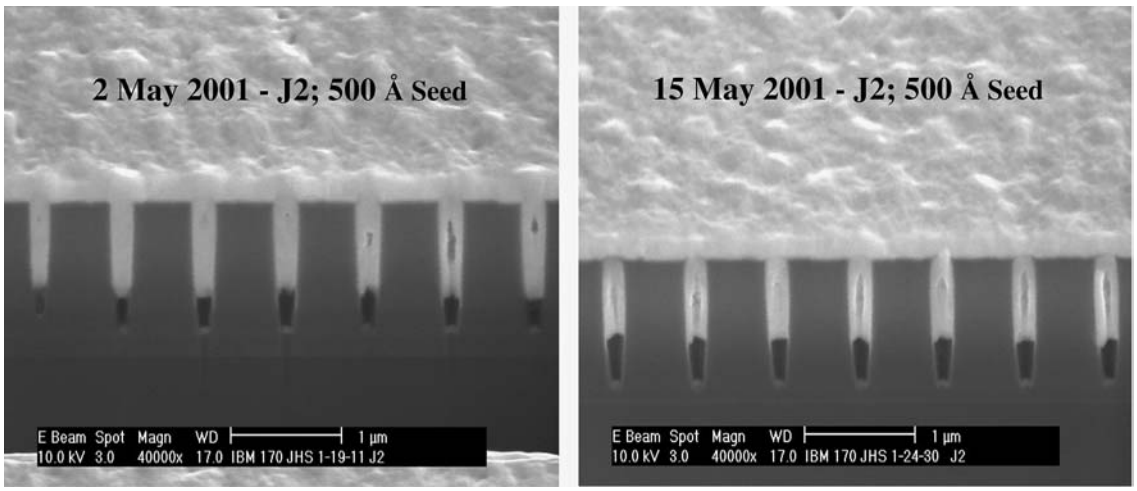

Fig. 1. FIB cut and SEM images of nonrepaired J2 vias.

avail it to seed repair applications include the alkaline nature of the plating bath chemistry (which prevents seed dissolution), the lack of process rate dependence on electrical continuity through existing seed to plated surfaces, and the ability to reduce copper oxides to copper metal. For these reasons, electroless copper is an ideal choice for uniform conformal seed repair across large substrates with high initial electrical resistance.

A different wet process seed repair method is electrodeposition from alkaline copper plating baths [7]. Some alkaline baths, such as copper pyrophosphate, have been widely used in the printed circuit board industry. Others, including EDTA–Cu or Cu–amine baths, although well known, are less widely used. In addition to the alkalinity of these baths, the low concentrations of strongly complexed copper shifts the copper reduction potential to extremely cathodic values. In turn, the high cathodic potentials required for copper deposition may be capable of reducing copper oxides to copper metal [6]. The low copper concentration has the additional benefit of improving thickness distributions between the centre and edge of resistive wafer surfaces [9]. However, high cathodic overpotential are also well known to evolve hydrogen even in alkaline solutions.

In this study PVD copper films of 250, 500, 750 and 1500 Å were initially deposited in 6:1 AR, 0.18 μm vias. The PVD films were processed through alkaline electroplating baths to form repair layers. Characteristics of the repaired seed layers and their resulting fill behaviour were studied.

2. Experimental details

Both pyrophosphate and EDTA alkaline baths were used. The pH of the pyrophosphate baths were generally not controlled using additional reagents (i.e., the buffering nature of the pyrophosphate ligands was used to control the pH). Otherwise, solution pH was controlled through addition of KOH or TMAH. Copper sources were copper pyrophosphate for the pyrophosphate bath and copper sulfate for the EDTA baths. A copper anode was used for all experiments.

Following repair, all wafers were electroplated in acidic copper sulfate baths which have been developed to provide accelerated bottom-up fill of well-seeded structures. In addition to the ligand type (i.e., EDTA and pyrophosphate), additional process parameters studied include: current density range 0.35–35 mA cm^{-2}; repair seed thickness 60–~500 Å; solution pH range 7–13; copper concentration range 10–100 mM; ligand-to-metal ratio range 1:1–5:1; solution temperatures 22 and 38 °C; rotation rate 20 and 100 rpm; and time between repair and electrofill ranging from seconds to six days.

Sheet resistance measurements of electrolytically deposited films on unpatterned 200 mm wafers were used to estimate the repair layer thickness deposited within the test features, 0.18 μm vias used in all fill studies. Copper coverage in vias was also quantified following repair using high magnification SEM of vias prepared by cleave or ion beam cuts.

3. Results and discussion

3.1. *Electrolytic repair impact on seed surface*

Figures 2 and 3 show SEM images of Cu metal coverage at the top and base of cleaved 6:1 AR vias at PVD thicknesses of 250 and 750 Å only, and following 75 and 250 Å seed repair. The electrolytic repair layer was deposited at 1.0 A using a pH 9.9, 1.25 g L^{-1} Cu, 14 g L^{-1} EDTA, and $T = 22$ °C electrolyte. At a PVD seed thickness of 250 Å a thin (<50 Å) and agglomerated layer of copper is observed on the top sidewall (Figure 3) of the vias. Near the base of the vias (Figure 2) it is not possible to resolve any Cu seed coverage through 250 000 × SEM examination following 250 Å PVD seeding alone. When PVD thickness is increased to 750 Å, more continuous and smooth

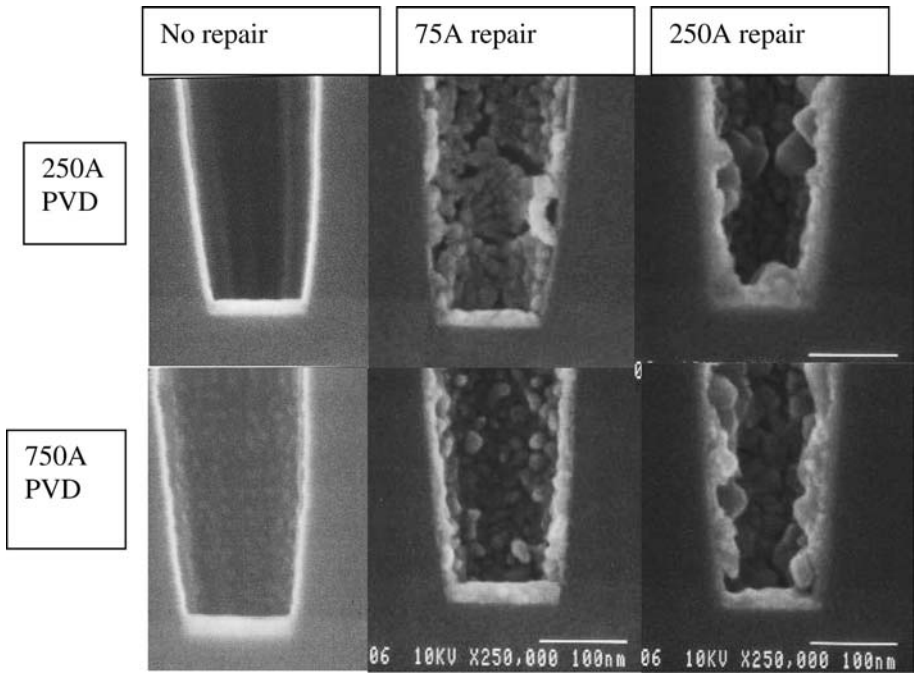

Fig. 2. Cleave SEM images of the base of 6:1 AR vias seeded with 250 and 750 Å Cu PVD without seed repair and following 75 and 250 Å repair in an EDTA bath.

copper coverage is noted on the top sidewall of the via and small islands of PVD seed are noted on the sidewalls near the base of the via.

After 75 Å electrolytic seed repair the coverage of copper inside the vias is seen to generally increase in thickness and to develop a rougher surface morphology. Near the via base, the 75 Å seed repair layer on 250 Å seed is discontinuous and not strongly adherent and appears to be propagating from discreet growth sites. On the upper via sidewall, the 75 Å seed repair layer on 250 Å seed is continuous and adherent but shows a rougher surface morphology. On the 750 Å PVD seed, the 75 Å repair layer is continuous and adherent. The coverage is very rough near the via base, but somewhat smoother on the initially smooth upper sidewall. When repair thickness is increased to 250 Å the coverage of

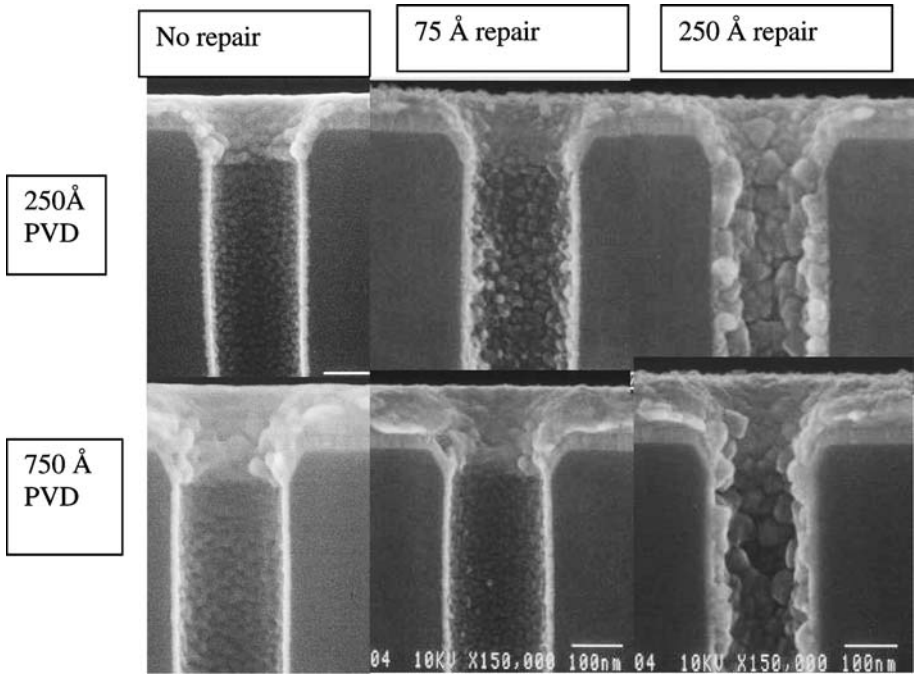

Fig. 3. Cleave SEM images of the top of 6:1 AR vias seeded with 250 and 750 Å Cu PVD without seed repair and following 75 and 250 Å repair in an EDTA bath.

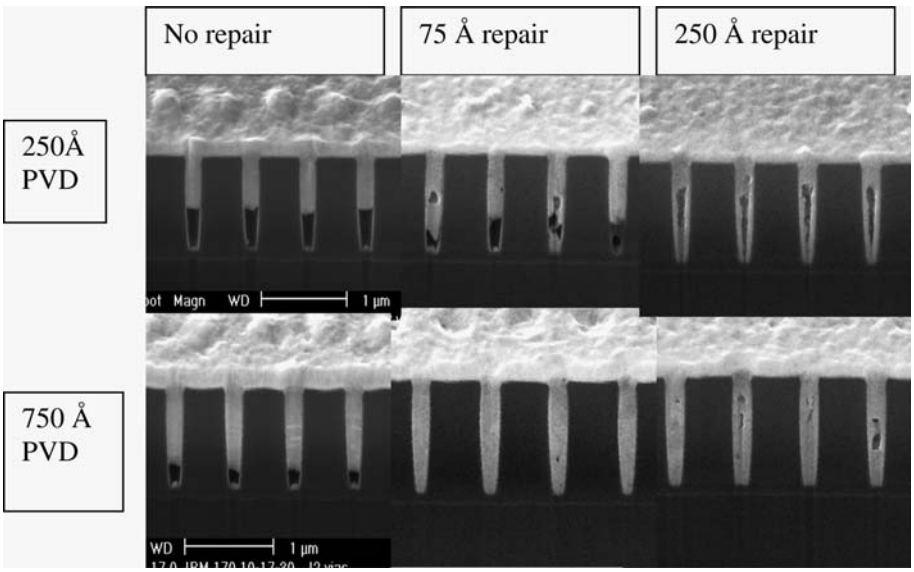

Fig. 4. Fill results in standard acidic electrofill bath following repair at pH 9.9, 1.25 g L^{-1} Cu, 14 g L^{-1} EDTA, $T = 22$ °C, at 1.0 A.

copper is substantial and continuous but very rough on all surfaces within the via. Deposition results from the seed repair electrolyte appear to be consistent with nucleation and growth on areas of initially isolated and/or oxidized PVD copper islands within the vias.

3.2. *Fill performance following repair*

Figure 4 shows the fill results of 6:1 AR following plating in a bottom-up acidic electroplating bath for the seed and repair conditions shown in Figures 2 and 3. For the PVD seed alone large bottom voids corresponding to the areas of initially poor PVD sidewall coverage are observed for both 250 and 750 Å seed thicknesses. Filling results after 75 Å of seed repair on the 250 Å PVD seed show somewhat smaller bottom voids, but the repair process is clearly inadequate. Filling results after 75 Å of seed repair on the 750 Å PVD seed show a small lower centre void but no sidewall voids indicating dramatic improvement in sidewall coverage using the repair process. The presence of a lower centre void in one via indicates fill is still not initiating as rapidly as desired on the repair layer. When repair thickness is increased to 250 Å, no sidewall voids are seen using either 250 or 750 Å initial PVD thickness values, however, large centre voids are observed. In this case, the pinch-off of the vias due to the substantial repair thickness is preventing the completion of bottom-up fill. These results, along with studies of additional seed and repair thickness values indicate that repair thicknesses in the range of 50–150 Å and initial PVD seed thickness values of 500–750 Å were optimum for fill improvement in 6:1 AR 0.18 μm vias.

Evaluation of seed repair process conditions and solution compositions was carried out in a series of experiments, the results of which are summarized in Table 1 and typical filling results are shown in Figure 5. Results of repair attempts in a pyrophosphate bath are shown in Figure 6. The best filling result was obtained using a low repair current density (0.3 mA cm^{-2}) for 150 s in EDTA solutions with relatively low copper concentration (0.02 M) which were adjusted to between pH 8–11 using KOH. In addition, repair was effective only using relatively low mass transfer rate conditions such as 20 rpm wafer rotation. Under these conditions the 6:1 vias were usually filled without significant voids when 100–150 A repair was performed on 500–750 Å PVD seed. Any deviation outside this process window resulted in increased centre and sidewall voids.

Table 1. Summary of parameters evaluated and observed trends

Parameter	Trend
Complexing agent	EDTA was more effective than pyrophosphate.
Repair current	Current density in the range of 0.35 mA cm^{-2} was most effective.
Repair thickness	Repair layer thickness of ~100 Å was found most effective.
pH	Solution pH in the range of 8 to 11 was found effective.
Copper concentration	Copper concentrations no higher than 20 mM was effective.
Ligand:metal ratio	Ligand to metal ratios between 1:1 and 5:1 were effective using KOH, high ligand concentrations were effective using TMAH.
Temperature	Room temperature was more effective than elevated temperatures.
Mass transfer	Wafer rotation speed of 20 rpm was found effective, higher mass transfer rates degraded repair

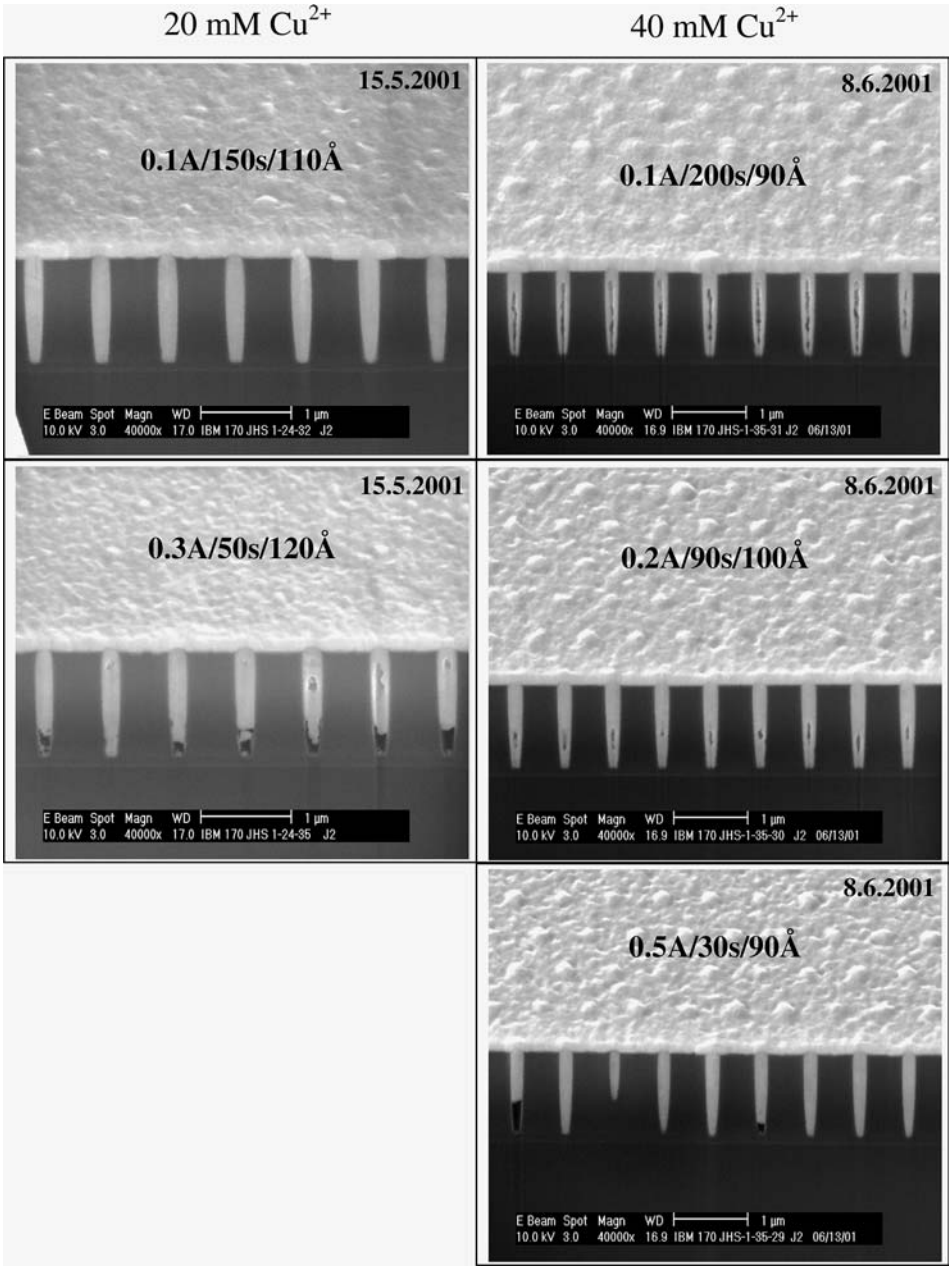

Fig. 5. Fill performance after repair in EDTA baths containing different copper concentrations and different repair current (0.1 A is equivalent to approximately 0.35 mA cm^{-2}). Ligand-to-metal ratio 1; solution pH 10; repair solution temperature 22 °C.

In Figure 5 it is seen that an increase in copper concentration from 20 to 40 mM eliminated repair viability at all current densities. Likewise, at 20 mM of Cu^{2+}, an increase of current density to 1.05 mA cm^{-2} is seen to have detrimental effects on the seed repair process. The difficulty in effecting repair was worsened when TMAH was used in place of KOH; the latter is an unacceptable potential source of contamination of alkali metals. In KOH, the effective current density range was 0.35–0.7 mA cm^{-2} and copper concentrations no higher than 20 mM. In TMAH, good repair was found only at 0.35 mA cm^{-2} and 10 mM Cu^{2+}. Figure 6 illustrates the difficulty in repair using the less polarizing pyrophosphate chemistry; bottom or centre seam voids are seen in all repaired 6:1 AR structures as well as in the 5:1 AR structures shown.

The results presented in Table 1 indicate that seed repair is most effective when sufficiently high cathodic potentials to cause copper oxide reduction to take place, but when excessive hydrogen evolution does not take place. High EDTA complexing agent concentrations combined with low copper concentration was most effective in achieving the overpotentials needed for oxide reduction. Hydrogen evolution under the otherwise strongly polarizing conditions was minimized by using a high solution pH and relatively low current density. The improved repair observed at lower RPM suggests the importance of intermediates in the repair

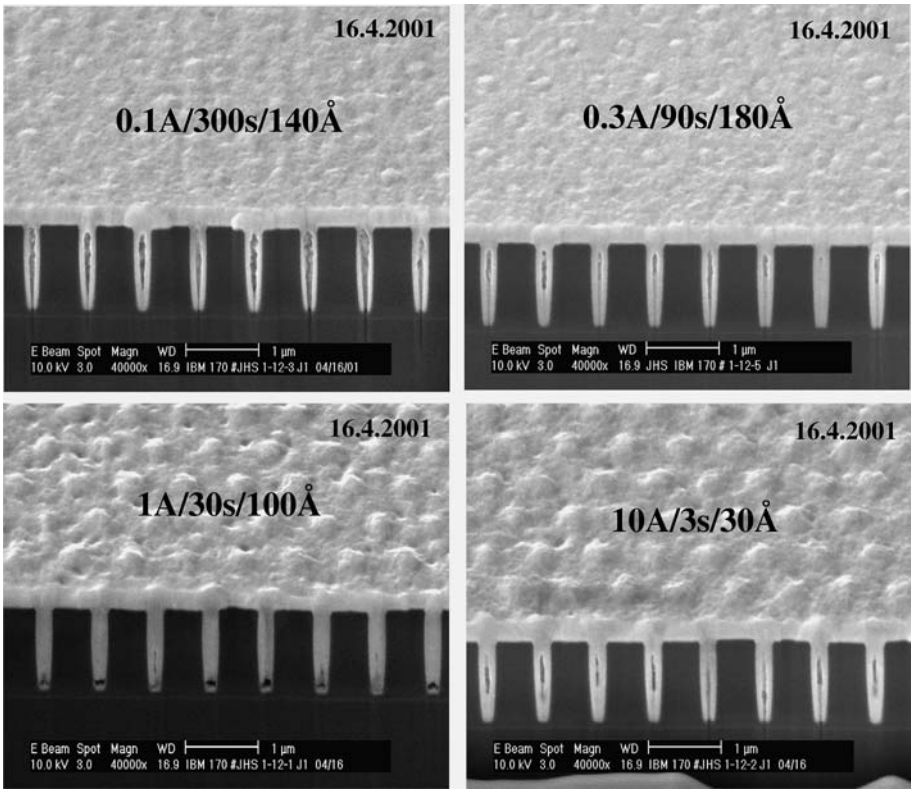

Fig. 6. Effect of repair current density in KOH (pH 9) and pyrophosphate and electrofilled in high acid UltraFill. Other experimental conditions: 20 mM Cu; 2.5 ligand-to-metal ratio; 20 rpm; 750 Å seed; 1 A for 11 s and 3 A for 30 s, hot entry during electrofill.

process (e.g., Cu^{+}), but the specific mechanism is not clear.

3.3. *Surface roughness and within-wafer uniformity*

In general, the copper surface of a blanket wafer was darkened after it has been subjected to an electrolytic repair process. In the presence of KOH, the surface was uniformly darkened. In the presence of TMAH, swirls were observed in addition to the general darkening of the surface. Figures 7 and 8 show typical optical images of blanket wafers subjected to two different electrolytic repair processes in TMAH. A generally rough surface topography, corresponding at least in part to the formation of pits in the repair layer, is evident. Larger pits appear to correlate with darker regions. In addition to the darkening of the surface, within wafer uniformity was typically >10% one sigma, as measured by sheet resistance, compared to sub-2.0% distributions normally measured for deposition in acidic baths. The wafer shown in Figure 7 has a wafer nonuniformity of 12.8% and the wafer shown in Figure 8 has a wafer nonuniformity of 11.7%. This nonuniformity may reflect variable current efficiency of the repair process and likely would indicate repair effectiveness variability across the wafer.

Variation of different process conditions (e.g., current density, rotation speed, wetting agent) within a range which provided substantial seed repair benefits was ineffective in eliminating the observed darkening of the surface. The morphology of surface irregularities was more irregular in the presence of wetting agents such as PEG600, as shown in Figure 9.

The morphology of 1 μm films electrodeposited on a 'repaired' and virgin blanket wafers are compared in Figure 10. The surface of the 1 μm film plated on a repaired seed layer shows surface depressions of varying sizes, some of which appear to be larger than the roughness features observed in the initially repaired seed

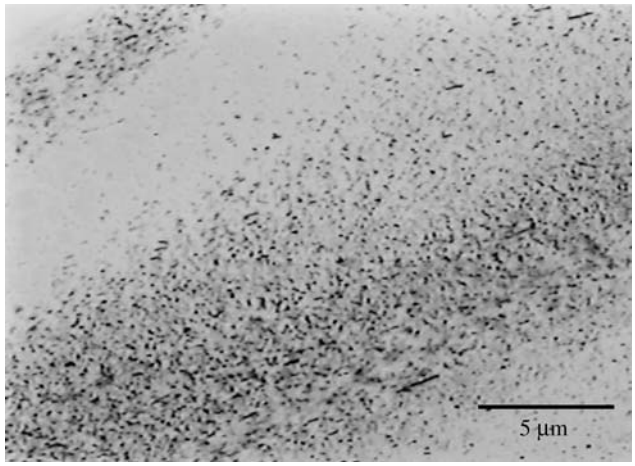

Fig. 7. Optical image across a swirl. The darker region appears to correlate with an area with a higher density of larger pits. Process conditions: 10 mM copper, 1.5 to 1 ligand-to-metal ratio, pH 9.6, 0.1 A for 300 s, 20 rpm, and room temperature.

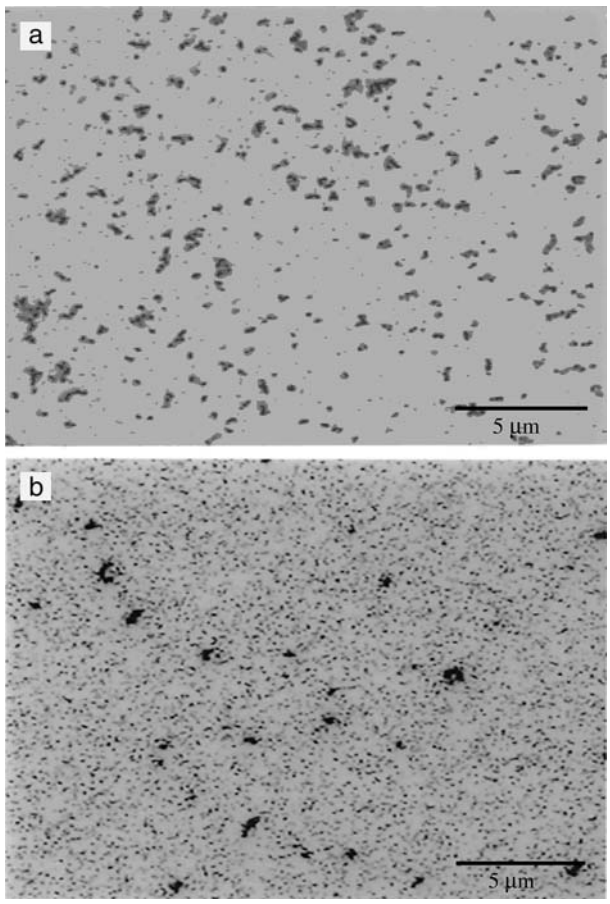

Fig. 8. Optical images comparing a 'dark' and 'light' regions. A darker region (top image) appears to correlate with an area with a higher density of larger pits. Process conditions: 10 mM copper, 1.5 to 1 ligand-to-metal ratio, 100 ppm PEG600, pH 9.6, 1 A for 60 s, 100 rpm, and room temperature.

layer. These depressions are believed to reflect both the initial topography of the repaired seed layer and variable wetting behaviour of the repaired seed layer in the acid copper bath.

Prewetting the blanket wafer prior to repair was also evaluated. It was found that pre-wetting reduced the degree of pitting in the repaired seed. However, upon deposition of a 1.0 μm film on the repaired blanket wafer, pits and protrusion defects were still found throughout the wafer surface. Qualitatively, more defects were found in regions with a thicker repaired layer.

3.4. *Mechanism of electrolytic seed repair*

The filling and surface roughness behaviour associated with seed repair under a variety of conditions allow further understanding of the mechanism of electrolytic seed repair. The repair process has the following steps that can occur sequentially or in parallel:

(i) Mass transport of complexed cupric ions to the electrode surface (within test structures and on the field).
(ii) Charge transfer across the interface resulting in the reduction of cupric to cuprous ions.
(iii) Further reduction of the cuprous ions to metallic copper.

Superior repair performance in EDTA solutions relative to pyrophosphate solutions is correlated, most likely, to the much stronger complexing characteristics of EDTA compared to pyrophosphate. A consequence of the stronger complexing ability of EDTA is that a more negative (cathodic) potential is required for the reduction of cupric to copper metal (Figure 11), and therefore the driving force for surface oxide reduction is also increased. The reduction of surface copper oxides to metal may both improve electrical connection to the via base and increase nucleation sites for subsequent copper electrodeposition. The standard reduction potential of Cu_2O to Cu in alkaline solutions is about −1 V vs SSE (CRC Handbook), and based on the voltammograms shown in Figure 11, it is evident that the reduction potential of Cu in the pyrophosphate bath is marginally (if at all) more cathodic than that required for reducing Cu_2O.

The result that better repair in EDTA solutions was observed at lower copper concentrations is also consistent with the hypothesis above, that is, larger thermodynamic barrier.

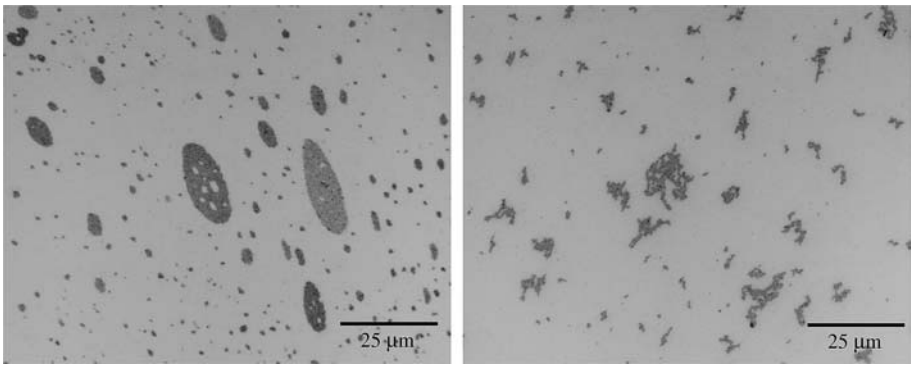

Fig. 9. Close-ups of pits on wafers processed in the absence (left) and presence (right) of PEG600. Aside from the shape of the outer boundary (smooth/circular vs jagged), the morphology of the pits is similar.

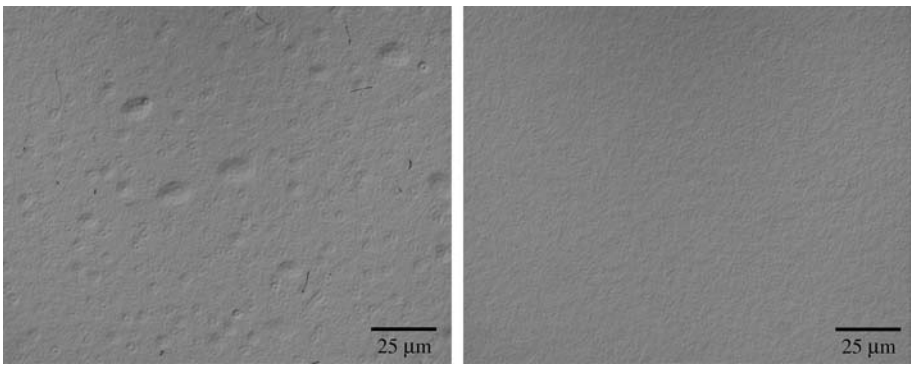

Fig. 10. Comparison of 1 μm films deposited using acidic electrofill baths on a 'repaired' (left) wafer and on a wafer with PVD seed alone.

The observation that higher EDTA-to-copper ratio was inconsequential in solutions where KOH was used to control the pH might simply be due to EDTAs preference for cupric against potassium ions. On the other hand, observation that more effective repair in TMAH was obtained only when a higher EDTA-to-copper ratio was used suggests interactions between the tetramethylammonium ions and the EDTA–Cu complex, which decrease the effective complexation strength of cupric ions and thus lower the thermodynamic barrier that cupric ions must overcome for deposition.

Step (ii) two appears to be important in differentiating between EDTA and pyrophosphate repair effectiveness as well as the dependence on cupric ion concentration.

In step (iii) the relevance of cuprous ion reduction kinetics to repair effectiveness is demonstrated by the improved repair efficiency at low mass transfer rates. The result that repair efficiency is diminished at high mass transfer rates indicates a relatively slow cuprous ion to copper metal reduction which can allow cupric intermediates to diffuse away from the interface prior to reduction.

The cause of the surface roughness and pitting may be related to hydrogen evolution or non-uniform corrosion of the seed surface. Both pitting and corrosion should increase with stronger complexing agents much like the overpotential for copper reduction increases.

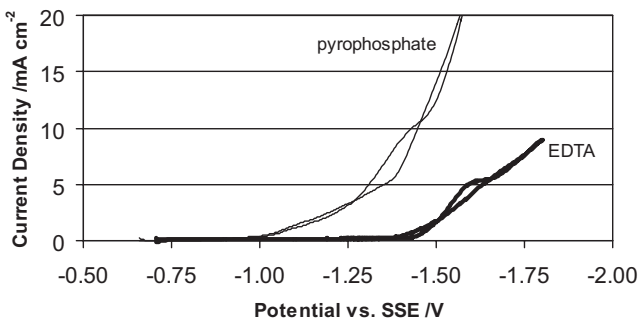

Fig. 11. Cyclic voltammograms of (a) 25 g L^{-1} copper pyrophosphate, 95 g L^{-1} potassium pyrophosphate, pH 8.7 and (b) 1.25 g L^{-1} Cu (from $CuSO_4$), 14 g L^{-1} EDTA, pH 9.9 (using KOH). Scan rate 2 mV s^{-1}. 300 rpm.

4. Conclusions

The effectiveness of electrolytic repair of initially discontinuous PVD copper seed in high aspect ratio vias generally increased as the degree of polarization during deposition from the repair solution increased. Mass transfer, pH, ligand concentration, current density, and metal ion concentration parameters all impacted the ability to form a repair layer which enabled subsequent fill in acidic plating baths. Under optimum repair conditions bottom voids were largely eliminated in 6:1 AR vias initially seeded with 500 Å of discontinuous PVD seed. Optimum conditions for seed repair took place at less than 100% current efficiency due to concurrent hydrogen evolution. However, these repair conditions also resulted in rough or pitted copper deposition on the wafer surface and high levels of measured defects in films subsequently plated in acid copper baths. As a result, it is concluded that both optimum electrolytic repair and deposition of defect-free copper films are not readily achieved in the same process, and thus practical implementation of electrolytic repair appears to be difficult and unpromising.

References

1. J. Reid and S. Mayer, *in* M.E. Gross, T. Gessner, N. Kobayashi and Y. Yasuda (Eds), Proceedings of the 'Advanced Metallization Conference', 1999 (MRS, Warrendale, PA, 2000), p. 53.
2. J. Reid, V. Bhaskaran, R. Contonlini, E. Patton, R.J. Jackson, E. Broadbent, T. Walsh, S. Mayer, J. Martin, D. Morrissey, R. Schetty and S. Menard, Proceedings of IITC, 24–26, May, 1999, pp. 284–286.
3. T. Ritzdorf, D. Fulton and L. Chen, *in* M.E. Gross, T. Gessner, N. Kobayashi and Y. Yasuda (Eds), Proceedings of the 'Advanced Metallization Conference', 1999 (MRS, Warrendale, PA, 2000), p. 101.
4. T.P. Moffat, J.E. Bonevich, W.H. Huber, A. Stanishevsky, D.R. Kelly, G.R. Stafford and D. Josell, *J. Electrochem. Soc.* **147** (2000) 4524.
5. J. Reid, S. Mayer, E. Broadbent, E. Klawuhn and K. Ashtiani, *Solid State Technol.*, **July** (2000) 86.
6. L. Chen and T. Ritzdorf, *Semicon. Fabtech*, July 2000, pp. 267–271.
7. Y. Lantasov, R. Palmans and K. Maex, Abstracts of the 'Advanced Metallization Conference' (MRS, Warrendale, PA, 2000), p. 30.
8. Y. Shacham-Diamand and V. Dubin, *Microelectron. Eng.* **33** (1997) 47.
9. K. Takashi, *J. Electrochem. Soc.* **147** (2000) 1414.